Chapter 9

**Hydrology of the Pacific Ocean**

The preceding chapter presented the currents of the Pacific Ocean essentially as wind-driven and treated temperature, salinity and other hydrographic properties as passive tracers, useful sometimes to demonstrate the effect of a current on hydrographic property fields but not responsible for the current's existence. This point of view is justified by the success of the Sverdrup model in explaining the major features of the oceanic circulation solely from the wind stress field, indicating that ocean currents are mainly wind-driven. On the other hand, our discussion of possible depths of no motion in Chapter 2 came to the conclusion that the Sverdrup circulation does not extend below 1500 m at most and that below that depth thermohaline forces must be responsible for water movement. We can use this fact to give our text some structure, by dividing the discussion of each ocean into two chapters. The first chapter concentrates on those elements of the circulation that are mainly wind-driven; thermohaline forces may modify details but are not the essential driving force. The second chapter addresses those elements of the circulation where thermohaline factors are responsible for the water movement or at least determine its direction.

This chapter discusses hydrographic property fields in the deep Pacific Ocean, using the distributions of temperature, salinity, and occasional other properties, to draw conclusions on currents below the direct influence of the wind. Since the driving agent for the thermohaline circulation is again the atmosphere, we begin the discussion with a brief review of surface conditions before turning to abyssal depths.

**Precipitation, evaporation and river runoff**

The region of highest precipitation in the Pacific Ocean as in all oceans is in the tropics where the southern and northern hemisphere Trade Winds meet, causing air to rise and release moisture. It occupies a narrow band in the vicinity of the equator and is characterized by weak and variable winds and heavy rainfall from cloud clusters associated with atmospheric convection and frequent electrical storms. This region is known in meteorology as the Intertropical Convergence Zone or ITCZ and as the Doldrums in the language of mariners.

In the Pacific Ocean the ITCZ was seen just north of the equator at 5°N in the last chapter, extending from South America to Indonesia and the Philippines. It is associated with annual mean rainfall in excess of 300 cm per year. Poleward of the ITCZ rainfall decreases towards the subtropics, reaching its absolute minimum of less than 10 cm per year in the coastal upwelling regions. As discussed in the last chapter, climatic conditions along the east and west coasts differ dramatically in the subtropics, and the subtropical rainfall minimum does not reach much below 200 cm per year in the west. In the northern hemisphere it cannot be identified west of 130°E where the band of high rainfall from the ITCZ bends northward to follow the Philippines Current and Kuroshio. The minimum is also very weak over the Coral and Tasman Seas. Further poleward, a rainfall maximum in both hemispheres is associated with the path of storm systems in the Westerlies (the Roaring Forties). In the northern hemisphere the band of high rainfall extends from Japan to Canada with values above 150 cm per year; in the southern hemisphere maximum values above 100 cm per year are found near 50°S.

A characteristic feature of the South Pacific Ocean is the existence of a second region of wind convergence in the tropics known as the South Pacific Convergence Zone or SPCZ. The last chapter showed it stretching southeastward from the ITCZ near the Philippines along New Guinea and the Solomon Islands towards Fiji and the Society Islands (Figure 8.5). Rainfall along the SPCZ is above 200 cm per year in the west and still above 150 cm per year between 140 - 160°W. The SPCZ is the result of strong monsoonal atmospheric motion across the equator over the Australasian Mediterranean Sea and in the extreme west of the equatorial Pacific Ocean, which causes the Trades to depart from their easterly direction on approaching Australia. During southern winter the southern hemisphere Trades are deflected toward the equator, establishing a convergence with winds coming in from the southeast (Figure 1.2b). During southern summer, when the Australasian monsoon extends weakly into the Coral Sea, air flow across the equator is from the north, and the southern Trades north of 20°S are deflected toward the pole (Figure 1.2c), again producing a convergence. The SPCZ is strongest during this season. It is seen that the SPCZ reflects the eastern limit for the influence of the monsoon system over the Indian Ocean on atmospheric conditions in the South Pacific Ocean.

Since over most of the Pacific Ocean evaporation varies much less than precipitation, the precipitation-evaporation balance (*P-E*; Figure 1.7) closely resembles the rainfall pattern. The SPCZ is evident as a ridge of high *P-E* values, as is of course the ITCZ. The contrast between the zonal uniformity in the northern hemisphere and the marked difference between the eastern and western South Pacific Ocean is remarkable. The increase of *P-E* values poleward of the subtropics is seen in the northern hemisphere. The corresponding increase in the southern hemisphere does not come out clearly in the figure due to lack of ship observations in this rarely travelled region.

Few rivers shed their waters into the Pacific Ocean, and the few that do have very small catchments. The largest rivers all enter the marginal seas along the western rim of the North Pacific basin, where they have a strong impact on the hydrography. This raises the *P-E* values of the marginal seas above the values found in the open ocean at comparable latitudes; these aspects will be discussed in more detail in Chapter 10. In the Pacific Ocean proper, the only evidence for significant contributions to the *P-E* balance from river runoff is seen along the Canadian coast. Although the rivers coming down from the mountain ranges are small they are numerous; their combined freshwater output of 23,000 m$^3$ s$^{-1}$ is comparable to that of the Mississippi River and constitutes about 40% of all freshwater input into the northeast Pacific Ocean (Royer, 1982). In the southern hemisphere river catchments are restricted by the Andes in the east and the Great Dividing Range of Australia in the west, so river contributions are negligible.

A major contribution to Pacific rainfall comes from atmospheric moisture imported from the north Atlantic Trade Winds. In the southern hemisphere the moisture collected from evaporation over the Atlantic Ocean is released as rain over the Brazilian rainforest and returns to the sea through the Amazon river. The land barrier of Central America, while receiving plenty of rain and nurturing luxurious rainforest, is not broad enough to catch all the moisture collected by the northern hemisphere Trades. The Atlantic Ocean therefore suffers a net freshwater loss across the land barrier, while the Pacific Ocean experiences a freshwater gain. This increases the salinity of the North Atlantic and decreases the salinity of the North Pacific Ocean. The resulting salinity difference between the two oceans has important consequences for the world climate. This aspect will be discussed in detail in Chapters 18 and 20.

## Sea surface temperature and salinity

The distribution of sea surface salinity (SSS, Figure 2.5b) mirrors the *P-E* distribution closely. The ITCZ is seen as a band of low salinity along 5 - 10°N. The SPCZ is evident as an extension of the tropical low salinities from New Guinea to Fiji. Minimum salinities in the ITCZ/SPCZ system occur in the Gulf of Panama, where salinity drops below 33.0 in the annual mean. This water originates from the North Equatorial Countercurrent, which crosses the Pacific Ocean eastward under the heavy rains of the ITCZ and arrives in the east with substantially reduced salinities. Weak currents in the Gulf of Panama expose the water further to the heavy rains produced by the import of Atlantic moisture. Eventually the diluted water exits into the North Equatorial Current and - via the Kuroshio - into the northern subtropical gyre. As a result the surface layer of the North Pacific Ocean is significantly less saline than that of the South Pacific Ocean.

The centres of the subtropical gyres coincide with the region of negative *P-E* or strong evaporation and are therefore characterized by high salinities. The salinity maxima are shifted somewhat to the west from the *P-E* minimum. This can be explained by the observation that winds in the centre of the gyres are weak and currents sluggish, so evaporation occurs over a longer time span than in the faster flowing eastern boundary currents.

Poleward of the subtropical gyres SSS decreases again, particularly in the northern hemisphere where the effect of ice melting from glaciers is felt along the Canadian and Alaskan coast. Salinities are also very low in the marginal seas along the western coastline. The influence of the Arctic Mediterranean Sea is seen in very low SSS values in Bering Strait.

The outstanding feature in the sea surface temperature (SST) is the expanse of very warm water in the western equatorial region. The contouring chosen for Figure 2.5a shows it with SST values higher than 28.0°C. Highest temperatures are encountered between eastern New Guinea and the equator where the annual mean is above 29.5°C. Annual mean temperatures are above 29.0°C between 10°N and New Guinea and the Solomon Islands and extend eastward along the SPCZ to 170°W. The thermal equator follows the ITCZ from 5°N in the west to 15°N in the east, with annual mean SST values generally above 27.0°C. The very high temperatures associated with the SPCZ and ITCZ are remarkable because they occur in a region of maximum cloud cover (Figure 8.5) which limits direct atmospheric heating. However, this effect is outweighed by the fact that the winds are weak over this region during most of the year (Figure 1.2), so there is little evaporative cooling.

The general poleward decrease of surface temperature produces a zonal orientation of most isotherms. Marked departures from zonal SST distribution are observed in the coastal upwelling regions. The Peru/Chile upwelling region stands out in this regard because it prevails strongly throughout the year. In the northern hemisphere the effect of coastal upwelling on the climatological mean SST is much weaker because the Californian upwelling is restricted to spring and summer. It is worth remembering when looking at Figure 2.5a that it is based on heavily smoothed data and cannot display features on scales much smaller than 700 km. The meridional orientation of the isotherms along the eastern coast is therefore more a result of equatorward advection of cold water in the Peru/Chile and California Currents than a direct consequence of coastal upwelling. But the cold water that upwells on and near the shelf is eventually transported offshore in the subtropical gyre and thus contributes indirectly to the lowering of offshore temperatures seen in the large scale SST distribution.

In the western Pacific Ocean the isotherms depart from strictly zonal orientation as a result of advection in the western boundary currents. The effect is clearly seen in the northern hemisphere where the convergence between the Kuroshio and the Oyashio produces a crowding of isotherms at the Polar Front. Advection by the East Australian Current can also be seen in the SST distribution; but the effect is much weaker, since the current has a much smaller transport and most of the current's energy is contained in its eddies.

**Abyssal water masses**

Although the Ross Sea, an important formation region of bottom water for the world ocean, is located in the Pacific sector of the Southern Ocean, the abyssal waters of the Pacific Ocean are renewed very slowly. This is primarily a result of topography: Arctic Bottom Water access is blocked by the very shallow Bering Strait, while most of the Antarctic Bottom Water produced in the Ross Sea is prevented from flowing north by the combined action of the Circumpolar Current and the Pacific-Antarctic Ridge and escapes through Drake Passage. The deep basins of the Pacific Ocean are therefore filled from the west. This is evident from the distribution of near bottom potential temperature in Figure 9.1 which shows *Antarctic Bottom Water* (AABW) entering south of New Zealand with potential temperatures below 0°C and moving eastward. Formation of AABW in the Ross Sea is indicated by a region of water colder than -0.5°C. The figure indicates three entry routes of AABW into the Pacific basins. All originate from the northern flank of the Circumpolar Current and therefore carry AABW in the form of Circumpolar Water; some authors therefore prefer that term for the bottom water of the Pacific Ocean. The western route, northward flow east of Australia, is blocked by topography near 20°S and of little importance outside the Tasman and Coral Seas. The eastern route, inflow along the East Pacific Rise east of 110°W, is blocked by the Chile Rise near 40°S and thus, too, does not contribute to bottom water renewal of most basins. This leaves the central route as the major point of supply. AABW enters the Southwest Pacific Basin east of the New Zealand Plateau and Chatham Rise and spreads gradually northward until it enters the Northwest Pacific Basin through the Samoa Passage (about 10°S, 169°W, east of the Tokelau Islands) and finds its way into the basins west of the Mariana Ridges through narrow deep passages. Most of this flow takes the form of narrow western boundary currents below 3500 m depth. In contrast, the vast expanse of the Northeast Pacific Basin is most likely renewed by uniform sluggish eastward flow.

The existence of western boundary currents above the ocean floor is demonstrated more convincingly in a vertical east-west section across the South Pacific Ocean (Figure 9.2). The observed rise of the isotherms against the western coast at depths below 4000 m is consistent with a northward "thermal wind" in which speed increases with depth (Rule 2a of Chapter 3). The feature is seen both in the Tasman Sea (150°E) and along New Zealand (165°W). The boundary current associated with the East Pacific Rise cannot be seen in the section, 43°S being too close to the Chile Rise to allow strong meridional flow there.

Detailed investigation of the circulation in Drake Passage reveals that circumnavigation of Antarctica is not the only route of AABW into the Pacific Ocean. The most direct route, from the Weddell Sea *westward* through Drake Passage, is taken by some 2 Sv of Weddell Deep Water. The water enters the Scotia Sea through a depression in the South Scotia Ridge near 40°W and follows the bottom topography along Antarctica in a narrow westward flow. This is clearly seen in the distribution of hydrographic properties (Figure 9.3). The

differences between values west and east of the Shackleton Fracture Zone indicate a warming of 0.5°C, a salinity increase of 0.04, and an oxygen loss of 0.4 ml/l for a circumnavigation; but cold, fresh, and oxygen-rich water is seen penetrating westward through a gap south of 61°S. The flow has been confirmed by direct current measurements which gave persistent speeds of up to 0.2 m s$^{-1}$.
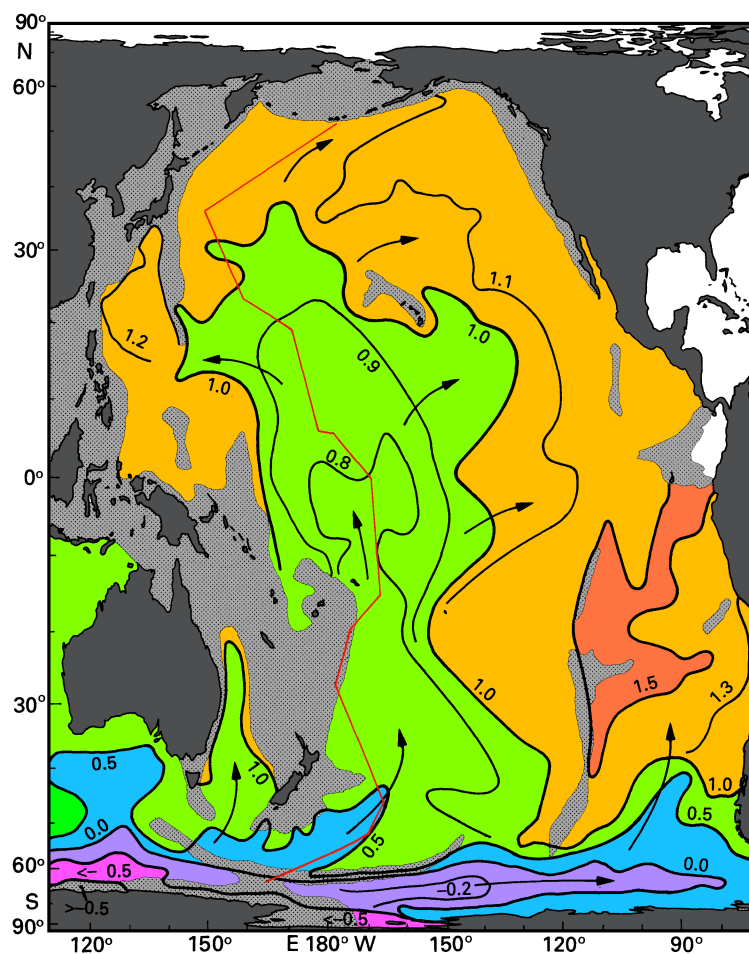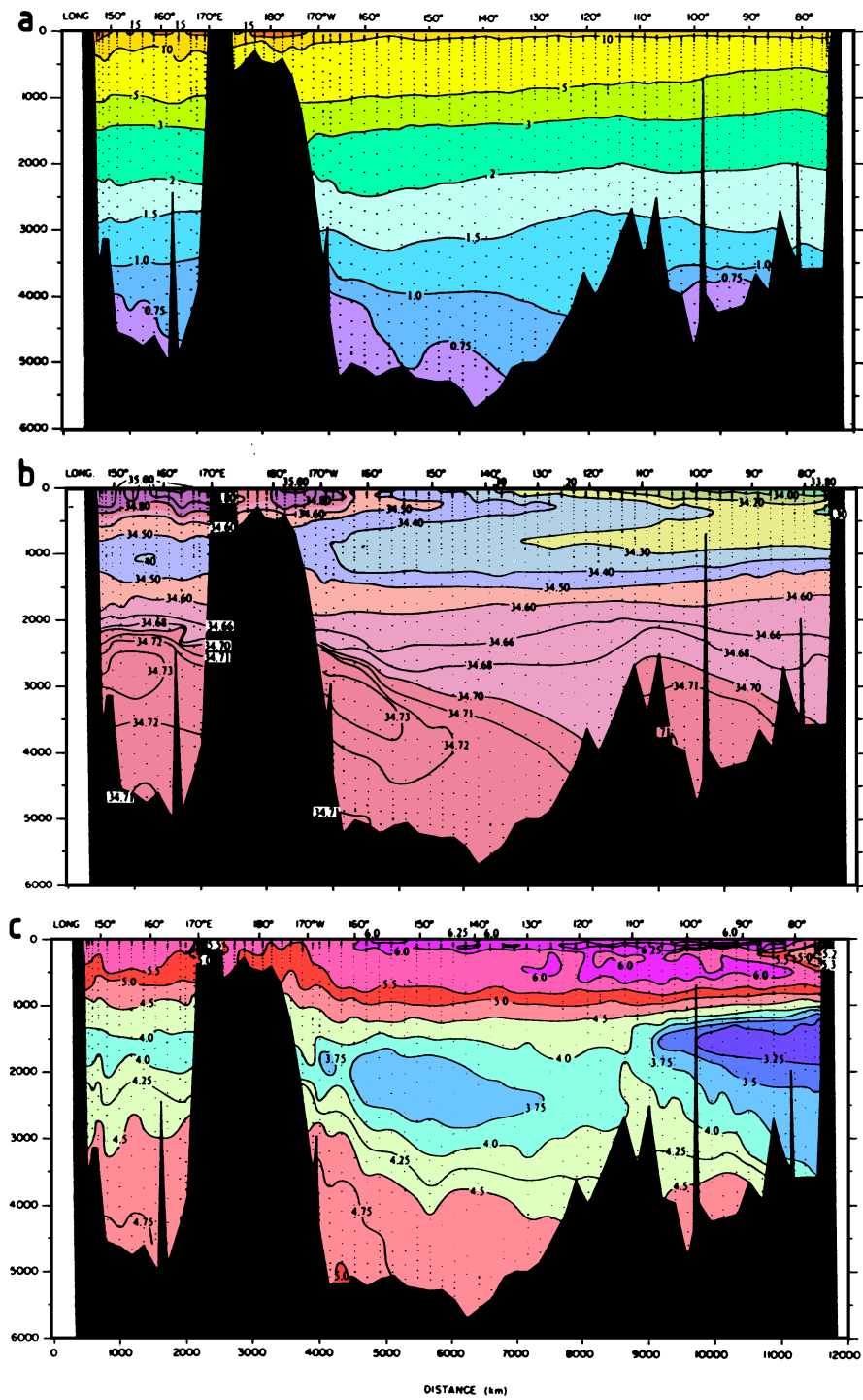
Fig. 9.1. Near bottom potential temperature (°C) in the Pacific Ocean. Arrows indicate the flow of Antarctic Bottom Water. Regions shallower than 3000 m are shaded. The thin line in the western basins gives the location of the section of Fig. 9.4. After Mantyla and Reid (1983).
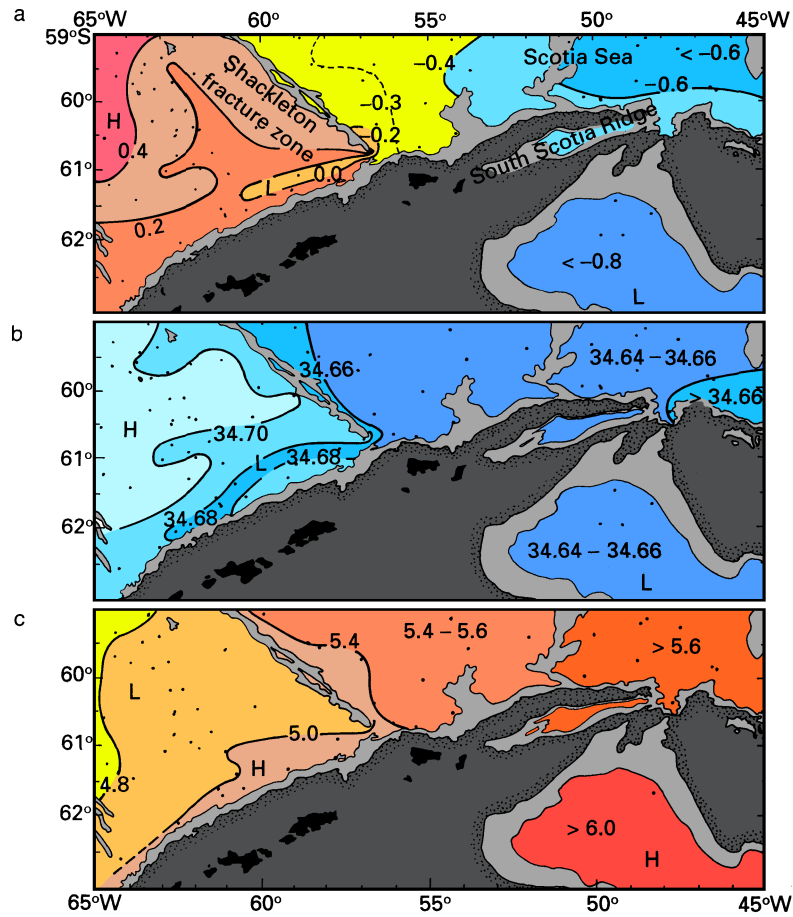
Fig. 9.3. Evidence for westward flow through southern Drake Passage. (a) Near bottom potential temperature (°C), (b) near bottom salinity, (c) near bottom oxygen content (ml/l). The 3000 m contour is shown as a thin line. Shading indicates depths less than 2000 m in panels a - c and land in the orientation panel. After Nowlin and Zenk (1988).

Fig. 9.2 (page 142). A zonal section across the South Pacific Ocean along 43°S. (a) Potential temperature (°C), (b) salinity, (c) oxygen (ml/l). From Reid (1986).

The three basins along the South American coast are separated from the remainder of the Pacific Ocean by topography and are therefore not reached by the AABW circulation. Figure 9.1 shows near bottom potential temperatures in the Peru and Chile Basins some 0.3 - 0.5°C warmer than elsewhere. This is the temperature above the Chile Rise, indicating that below the sill depth the Chile Basin is filled with water crossing the ridge from the south. The water then follows the Peru/Chile Trench along South America into the Peru Basin and continues into the Panama Basin, a small basin of near 3800 m depth blocked on all sides at the 2300 m level, with a sill depth in the trench of approximately 2900 m just south of the equator. Observations 100 m above the sill gave a mean inflow speed over a 17 day period of 0.33 m s$^{-1}$, which gives a rough transport estimate of 0.2 Sv, with a potential temperature of 1.6°C. By the time this amount of water leaves the Panama Basin through upwelling and outflow above the 2300 m level it has acquired a potential temperature of 1.9°C, while its salinity remains unchanged. This indicates that the heat required to raise the temperature by 0.3°C is not so much derived from mixing with the waters above (which would affect the temperature and salinity) but from geothermal heating in the Galapagos sea floor spreading centre. This places the Panama Basin amongst the few ocean regions where geothermal heating provides an important contribution to the heat budget. Geothermal heating has also been verified in the Northeast Pacific Basin (Joyce *et al.*, 1986), but the increase in bottom temperature does not exceed 0.05°C in that case.

Figure 9.4 gives a meridional hydrographic section through the western Pacific Ocean. The outstanding feature is the uniformity of water properties below 2000 m depth. The circulation in this region is very sluggish. AABW is slowly advected from the south, mixing with the water above, its aging being indicated by the northward decrease of oxygen content. The oldest water is found in the northern hemisphere, just below the tongue of well oxygenated low salinity Intermediate Water (to be discussed below), where oxygen values fall below 50 $\mu$mol kg$^{-1}$ (about 1.1 ml/l). Measurements of $^{14}$C indicate that more than 1000 years elapsed since this water was in contact with the atmosphere. In contrast to the North Atlantic Ocean which contributes to the formation of the oceans' abyssal water masses, no deep or bottom water is formed in the North Pacific Ocean. This is not only the result of Bering Strait blocking deep communication with the Arctic Mediterranean Sea; In the North Atlantic Ocean, Deep Water would still be produced if the connection between the Arctic Mediterranean Sea and the Atlantic Ocean were closed, by deep winter convection in the Greenland and Labrador Seas. In the North Pacific Ocean such deep winter convection is inhibited because its surface salinity is much lower than that of the North Atlantic Ocean (Figure 2.5b). This reduces the surface density sufficiently to prevent it from exceeding the density below the mixed layer even in winter. Surface salinity in the northern Pacific Ocean is thus of immense importance for the global oceanic circulation and consequently for climate. This aspect will be taken up again in the last chapters.

The distribution of oxygen (Figure 9.4c) indicates the penetration of AABW into the northern hemisphere below 3000 m and active circulation associated with the spreading of Intermediate Water above 1000 m depth. In the northern hemisphere, water in the depth range 1000 - 3000 m does not participate much in the circulation; its properties are determined nearly entirely through slow mixing processes. This water is usually called *Pacific Deep Water* (PDW), in analogy to the North Atlantic and Indian Deep Waters which occupy the same depth range. Identification of the oldest water in the Pacific Ocean as a distinct water mass is justified but requires some explanation in view of our water mass definition of Chapter 5.
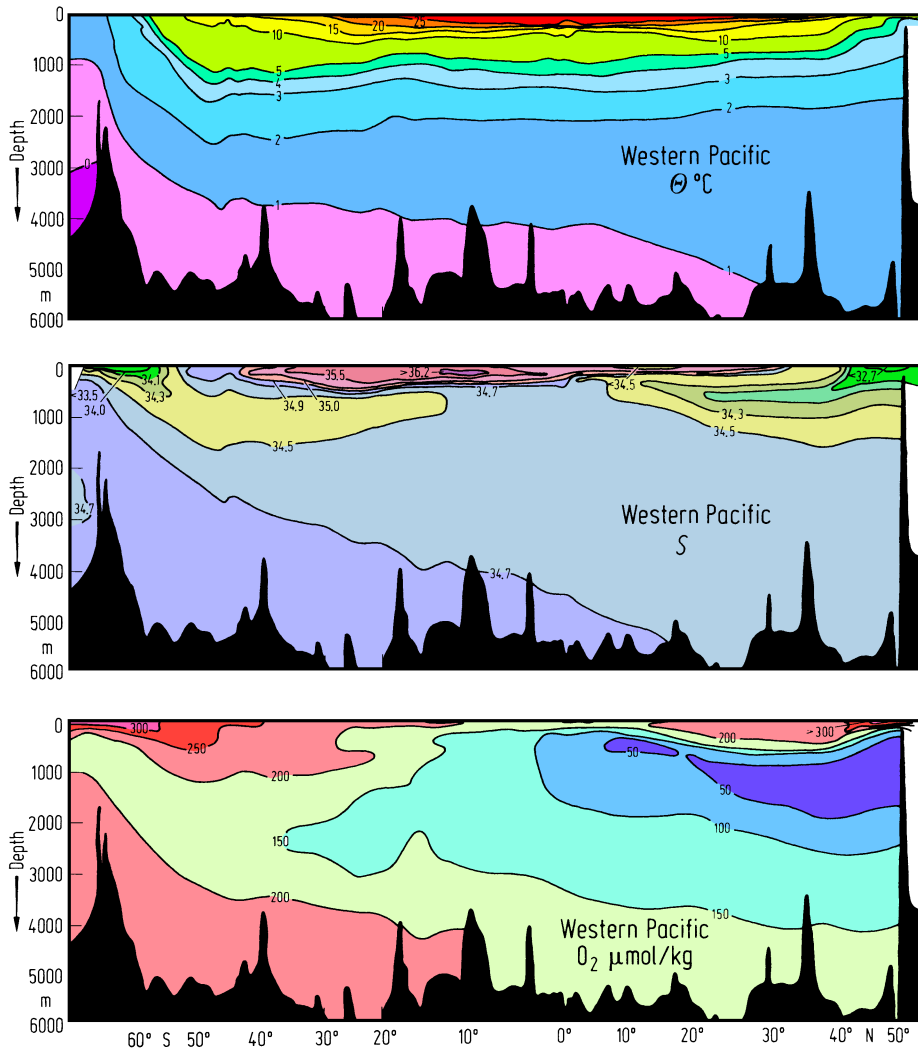
Fig. 9.4. A north-south section across the Pacific Ocean in the west. (a) potential temperature (°C), (b) salinity, (c) oxygen ($\mu$mol/kg; an approximate conversion to ml/l, correct near $\Theta = 5°C$, S = 34.45, is 100 $\mu$mol/kg = 2.24 ml/l). From Craig *et al*. (1981). See Fig. 9.1 for location of section.

Figure 9.5 compares Deep Water properties of the three oceans. The different character of Atlantic, Indian, and Pacific Deep Water comes out clearly. North Atlantic Deep Water is formed at the surface in a region of very high surface salinity and is therefore seen in the T-S diagram as a salinity maximum between Bottom and Intermediate Water. The characteristics of Indian Deep Water will be discussed in Chapter 12; in essence, it is North Atlantic Deep Water (NADW) advected into the Indian Ocean and there-fore given a different name. In the T-S diagram it is again present as a salinity maximum, with T-S values very

close to those of North Atlantic Deep Water east of 40°E, the maximum being eroded further east and north through mixing with the waters above and below (Figure 9.5 shows maximum salinity just above 34.7 near 70°E). In contrast, the T-S values of Pacific Deep Water do not depart very much from the mixing line between Bottom and Intermediate Water except in the vicinity of the Southern Ocean, where a faint salinity maximum indicates that traces of North Atlantic Deep Water, having crossed the Indian Ocean under the name of Indian Deep Water, are entering the Pacific Ocean from the Great Australian Bight. It is thus seen that the constituents of Pacific Deep Water are Antarctic Bottom Water, North Atlantic Deep Water, and Antarctic Intermediate Water. This mixing process constitutes the common formation history of all Pacific Deep Water.
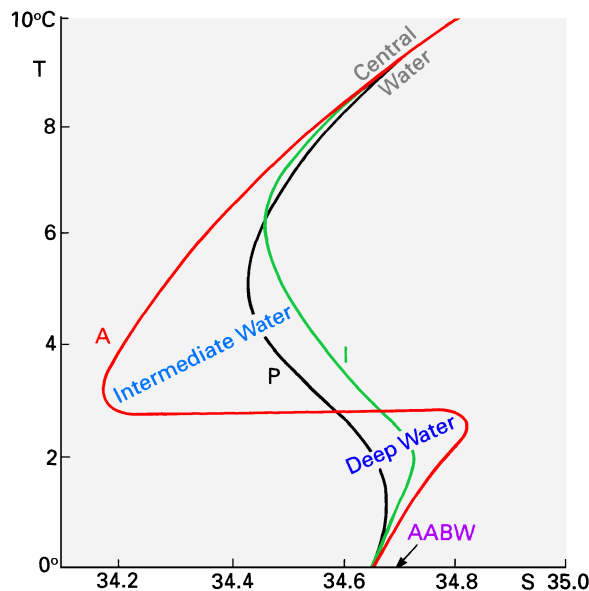


Fig. 9.5. A comparison of T-S diagrams from the three oceans in the southern hemisphere.

A: Atlantic Ocean (at 41°S),
I: Indian Ocean (at 32°S, 70°E),
P: Pacific Ocean (near 43°S, 120°W).
AABW: Antarctic Bottom Water.

Evidence for a contribution of NADW to Pacific Deep Water can be seen in Figure 9.2b which shows a weak salinity maximum at and below 3000 m depth, indicating that some NADW enters in western boundary currents along the continental rises of Australia and New Zealand. Lateral mixing must be important along the path, as the horizontal extent of the maximum is far too large to indicate the true width of the boundary currents. Figure 9.6 traces NADW from its formation region through the Atlantic and Indian Oceans into the Pacific Ocean. The salinity maximum in the Pacific Ocean can be followed nearly to the equator where the extinction of NADW through conversion into PDW is complete. The path of NADW shown in the figure differs significantly from the recirculation path discussed in Chapter 7. It suggests NADW propagation into the Indian and Pacific Oceans without significant upwelling and water mass conversion (from NADW into AAIW) in the Southern Ocean. Since there is no exit for PDW from the north Pacific basins, it has to upwell into the overlying Intermediate Water; so conversion of NADW into Intermediate Water does occur eventually, but the details of the heat and salt budgets involved are quite

different for the two pathways. Figure 9.6 leaves no doubt that some NADW reaches the Indian and Pacific Oceans with the abyssal circulation. On the other hand, the discussion of Chapter 7 showed that deep upwelling and associated conversion of NADW into AAIW in the Southern Ocean is a dynamic necessity of the circumpolar circulation. The necessary conclusion is that the NADW recirculation is shared between both paths.
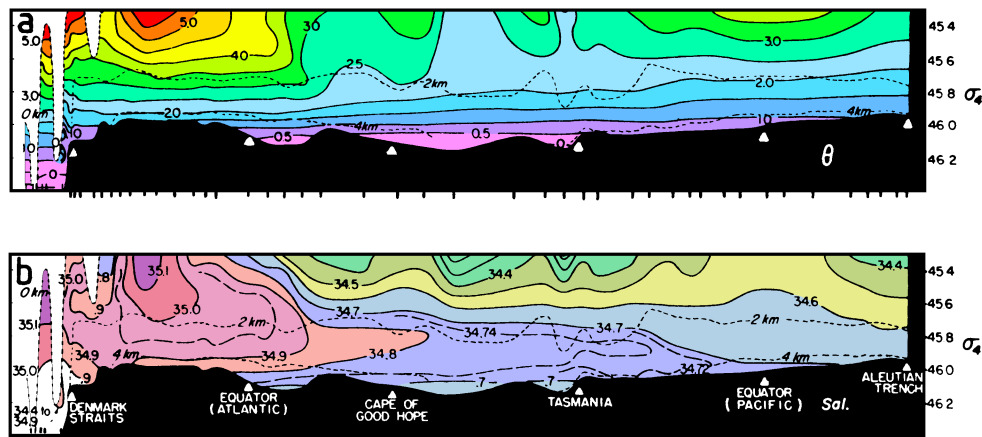


Fig. 9.6. A vertical section from the North Atlantic Ocean near Denmark Strait southward around southern Africa, then eastward through the southern Indian Ocean past Tasmania and New Zealand, then northward into the North Pacific Ocean. (a) potential temperature (°C), (b) salinity. The ordinate uses $\sigma_4$, the density a parcel of water would have if moved adiabatically to a pressure of 40,000 kPa (approximately 4000 m depth). Actual depths are indicated by broken lines. Tick marks along the bottom indicate station positions. From Reid and Lynn (1971).

The salinity minimum near 800 - 1000 m depth in both hemispheres indicates the presence of Intermediate Water. At this depth the movement of water no longer follows the deep circulation (northward movement in western boundary currents with slow return circulation through the eastern basins) but is part of the upper layer circulation which shows symmetry around the equator (broad equatorward flow in the subtropical gyres and poleward flow in the western boundary currents). Until very recently it was thought that *Antarctic Intermediate Water* (AAIW) originates from subduction along the Polar Front. Recent results (England *et al*., in press) indicate that much of the AAIW in the world ocean may form west of South America through convective overturning of surface waters during winter. It is then injected into the subtropical gyre, filling the southern subtropics and tropics from the east. *Subarctic Intermediate Water* (SIW) originates from the Polar Front formed between the Kuroshio and Oyashio in the western North Pacific Ocean, where it is formed mainly by mixing of surface and deeper waters (i.e. without direct contact with the atmosphere) and subducted into the subtropical gyre, filling the northern hemisphere south of 40°N again from the east. A map of salinity at the depth of the minimum (Figure 9.7) is somewhat indicative of Intermediate Water movement. Strong contrast between minimum salinities in the east and west is seen in the South Pacific Ocean. Numerical models of the oceanic circulation attribute this to a strong injection of new AAIW from the

winter convection region west of southern South America which is transported westward with the subtropical gyre, opposing the eastward flow of old AAIW advected from the west. The latter component is traced back to the winter convection region in the Atlantic Ocean (east of southern South America) by the models. Verification of these ideas in the field is required before we can be more definite on the reasons for the east-west salinity gradient at the level of the salinity minimum. Minimum salinities are much more uniform near the equator where AAIW and SIW meet and dissipate through upwelling, leaving only a faint trace of a minimum (Figure 9.4).
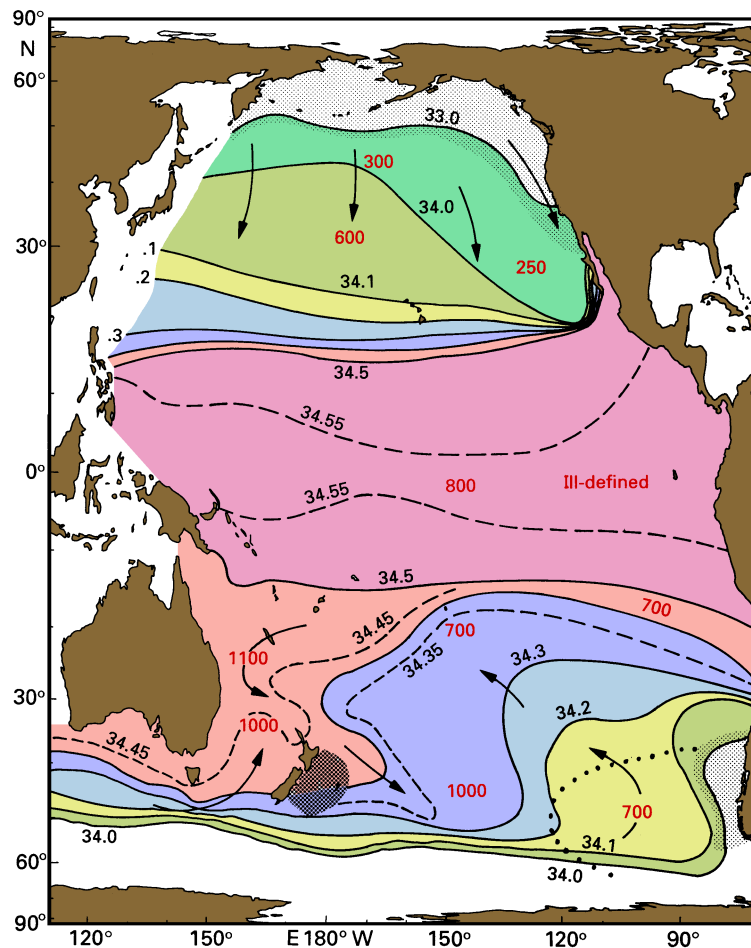


Fig. 9.7. Salinity at the depth of the salinity minimum, indicating the spreading of Intermediate Water. The depth of the minimum is also indicated; light shading indicates regions where the minimum is at the surface. The dotted line in the southeast marks a region where surface salinities are lower than those shown for the minimum at 700 m. East of New Zealand the water depth is too shallow for Intermediate Water to occur. Note that salinities between 33 and 34 are not contoured.

Movement of AAIW in the western South Pacific Ocean is strongly influenced by the topography. The presence of New Zealand results in AAIW entering the Tasman Sea along two paths. AAIW with minimum salinity less than 34.4 enters from the south, taking the shortest route from the Polar Front. It does not spread very far northward, however, being opposed by a second source of AAIW supply from the east. This water spreads westward through the Coral Sea, enters the Tasman Sea from the north and leaves it with the East Australian Current extension around the northern tip of New Zealand's North Island (It can be traced, through its slightly higher minimum salinity, along the northern flank of the Chatham Rise to about 160°W). T-S diagrams from the Tasman Sea often do not show the Intermediate Water as a broad salinity minimum in a smooth T-S curve but reveal a high level of finestructure and interleaving (Figure 9.8). The phenomenon has been observed in all oceans north of the Antarctic Polar Front (Piola and Georgi, 1982); but in the Tasman Sea it is found well north of the formation region of AAIW and further north than in all observations elsewhere. A possible explanation is that AAIW formation takes place in a number of regions along the Polar Front (e.g. in the South Atlantic and eastern South Pacific Oceans) and that its T-S properties vary slightly between different formation regions. The small inversions in the T-S curve would then indicate interleaving of AAIW from different source regions. Similar interleaving occurs in the formation region of SIW, suggesting Intermediate Water formation in distinct regions of the Polar Front of the northern hemisphere as well.
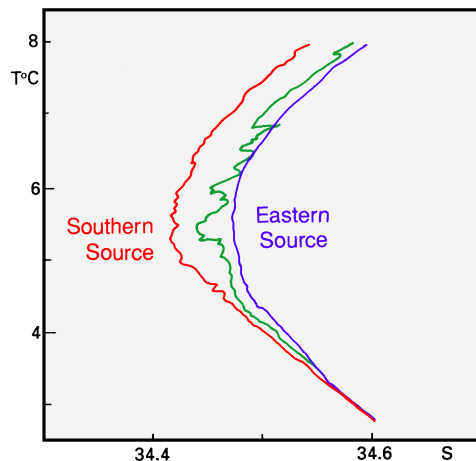


Fig. 9.8. T-S diagrams from the northern Tasman Sea near 28°S, showing stations with and without finestructure and interleaving at the level of Antarctic Intermediate Water. Interleaving is high over the Lord Howe Rise, which suggests increased turbulent mixing between the two sources over shallow ridges.

Since Intermediate Water originates from the Polar Fronts and joins the subtropical gyre circulation, it is not found in the subpolar gyre of the North Pacific Ocean. The water that occupies the depth range of Intermediate Water north of the Arctic Polar Front is called the Subarctic Upper Water. It is not restricted to subsurface layers but occupies the upper few hundred meters of the water column. Its discussion is therefore taken up again in the next section.

**Water masses of the thermocline and surface layer**

Chapter 5 explained how the water masses of the thermocline are subducted in the Subtropical Convergence (STC) and fill the upper kilometer of the ocean by spreading on isopycnal surfaces. The name Central Water was introduced in that chapter, and it was pointed out that these water masses are characterized by temperature-salinity (T-S) relationships that span a large range of T-S values in a well defined manner (see Figures 5.3 and 5.4). The principle is easily applied to the Indian and Atlantic Oceans, where it serves as a valuable guide to a physical interpretation. The thermocline of the Pacific Ocean, on the other hand, displays a variety of T-S relationships, and some care is required to identify associated water masses and processes. The existence of different T-S relationships for different parts of the Pacific Ocean is most likely due to its large size, in comparison to the other two ocean basins, which leads to variations of atmospheric conditions and therefore surface T-S relationships in the Subtropical Convergence.
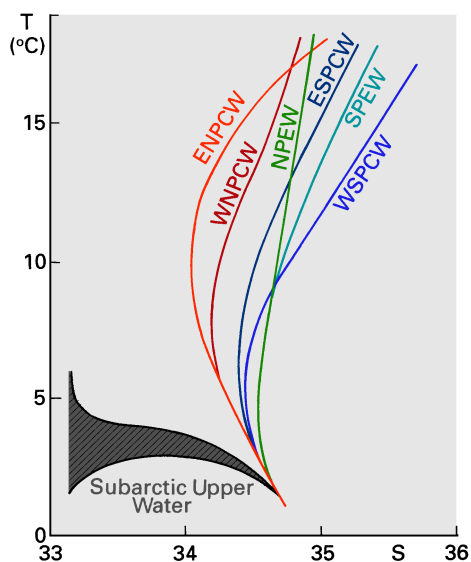


Fig. 9.9. Temperature-salinity relationships in the Pacific Ocean thermocline.

ENPCW:  Eastern North Pacific Central Water,
WNPCW:  Western North Pacific Central Water,
SPEW:   South Pacific Equatorial Water,
NPEW:   North Pacific Equatorial Water,
ESPCW:  Eastern South Pacific Central Water,
WSPCW:  Western South Pacific Central Water.

Six thermocline water masses can be distinguished in the Pacific Ocean (Figure 9.9). *Western South Pacific Central Water* (WSPCW) is the most saline; its T-S properties are virtually identical to those of Indian and South Atlantic Central Water, indicating identical atmospheric conditions in their formation regions. WSPCW is formed and subducted in the STC between Tasmania and New Zealand. Its occurrence is restricted to the region west of 150°W and south of 15°S (Figure 9.10). The transition to the fresher *Eastern South Pacific Water* (ESPCW) is gradual; but east of the transition, between 145°W and 110°W, the T-S properties of the thermocline are quite uniform and very close to the T-S curve labelled ESPCW in Figure 9.9, indicating that ESPCW is indeed a Central Water variety with its own formation history. Comparison with surface T-S diagrams across the Subtropical Convergence indicates that it is formed between 180° and 150°W (Sprintall and Tomczak, in

press). East of 110°W the Subtropical Front (the southern limit of the STF) weakens considerably, and advection of Subantarctic Upper Water in the Peru/Chile Current reduces the salinity in the thermocline. Salinities as low as 34.1 are found in the upper thermocline east of 90°W. This region, identified in Figure 9.9 as a "transition region" for lack of a better name, requires more study before its water masses can be properly described.
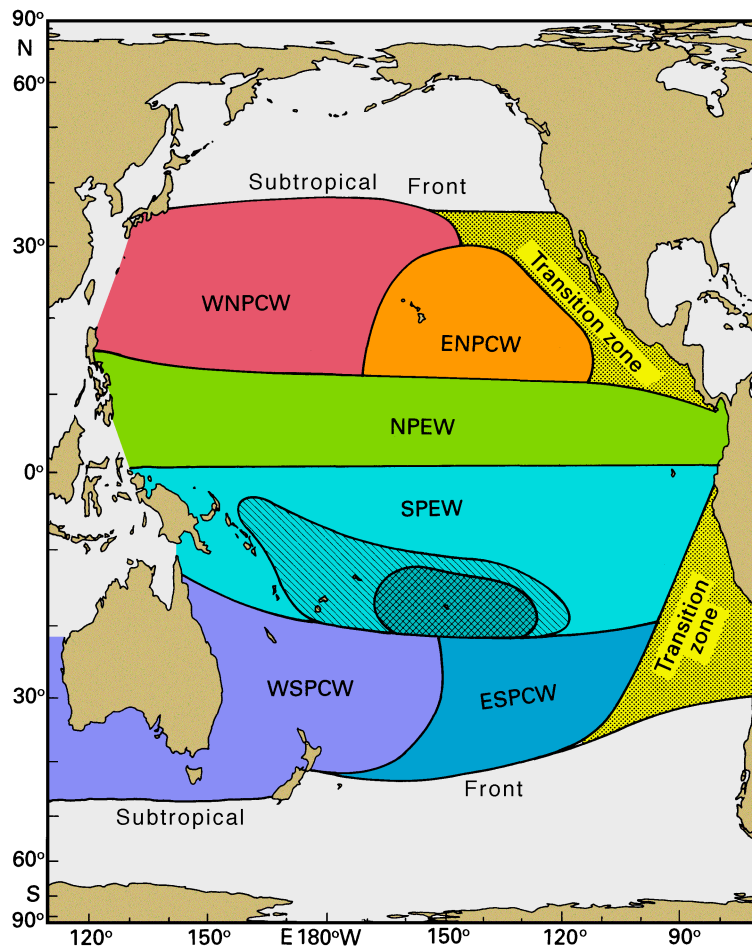


Fig. 9.10. Regional distribution of thermocline water masses in the Pacific Ocean. Shading in the region of South Pacific Equatorial Water indicates the areas where mean climatological salinity during August is above 36 at the surface (dark shading) and at 200 m depth (light shading). See Fig. 9.9 for more details and abbreviations.

The dominant water mass of the thermocline in the northern subtropical gyre is the *Western North Pacific Central Water* (WNPCW). It is formed and subducted in the northern STC. Sea surface salinities there are lower than those found in the southern STC, and

WNPCW is thus significantly fresher than the Central Waters in the south. Again, a second variety of Central Water can be distinguished in the east. *Eastern North Pacific Central Water* (ENPCW) is fresher than WNPCW in the temperature range below 17°C but more saline in the upper thermocline. This and the fact that the boundary between the two water masses near 170°W is quite distinct, indicates that ENPCW has its own formation history. Its low salinities at the lower temperatures are probably the result of mixing with Subarctic Upper Water; but the high salinities above 17°C are well above those of all water masses in the vicinity and can therefore only be generated at the surface. This places the formation region in the region of the surface salinity maximum just south of 30°N, where salinities in excess of 35 are found throughout the year (Figure 2.5b).

The largest volume of the Pacific thermocline is occupied by Pacific Equatorial Water, a water mass without equivalent in the other two oceans. At temperatures above 8°C it displays two varieties; both have T-S properties intermediate between those of Central Water found in the two hemispheres (Figure 9.9). Below 8°C their T-S properties merge into a single curve which eventually reaches T-S combinations outside the range of Central Water. The high salinities at these temperatures reflect the absence of Intermediate Water in the tropics and indicate that Equatorial Water has contact and mixes with Deep Water.
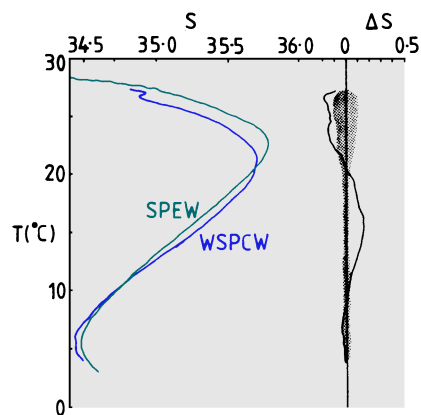


Fig. 9.11. T-S diagrams for WSPCW and SPEW derived from 42 CTD stations (37 for SPEW, 5 for WSPCW) in the eastern Coral Sea. The curve at the right is the salinity difference *ΔS* between the two water masses. The shaded area gives the standard deviation for salinity in both water masses. From Tomczak and Hao (1989).

The formation region of *North Pacific Equatorial Water* (NPEW) is at the boundary between the subtropical gyres and involves mixing in the Equatorial Countercurrent and in the Equatorial Undercurrent. Since both currents originate in the west, the water masses involved in the mixing are of the western variety. The T-S diagram indicates that NPEW is a mixture of WNPCW and SPEW, with the larger Central Water contribution in the upper thermocline. Mixing in the core region of the eastward components of the equatorial current system thus has to be regarded the common formation mechanism for all elements of this water mass; in other words, NPEW is one of the few water masses not formed through air-sea interaction. *South Pacific Equatorial Water* (SPEW), on the other hand, is partly formed by convective sinking of surface water in the tropics: South of the equator and east of 170°W (from the Polynesian islands to South America) evaporation exceeds precipitation (Figure 1.7), and sea surface salinity exceeds 36 throughout the year, making Polynesia the region with the highest salinity of the Pacific Ocean. The extent of the area for August is

shown in Figure 9.10, which also includes the area where the salinity is above 36 at 200 m depth. It is seen that the high salinities reach much further west in the thermocline than at the sea surface. The origin of these high thermocline salinities must be at the sea surface, since the highest salinity reached in the Subtropical Convergence and therefore found in Central Water does not reach 35.8. This leads to the conclusion that convective sinking through evaporation occurs in the Polynesian region, at sea surface temperatures of 26°C and above. Maximum temperatures and salinities are reduced during sinking and spreading by mixing; but even in the Coral Sea where maximum salinities have fallen off to 35.8 and less, SPEW can still be clearly identified at temperatures above 20°C by its higher salinity when compared with WSPCW (Figure 9.11). Below 20°C SPEW appears to be a mixture of WSPCW and ESPCW.

Although the differences in T-S values between SPEW and WSPCW are small, the boundary between the two water masses along 20°S in the central Pacific Ocean and about 15°S in the Coral Sea is quite distinct. This is borne out in Figure 9.11 which shows the small salinity differences between the two groups of stations as being well outside the standard deviation, i.e. the natural variability, of salinity in each water mass. Steric height and salinity distributions indicate that south of 15°S WSPCW is advected from the south-east, while north of 15°S SPEW enters the region from the east. It is worth noting also that at the upper level (where the temperature is well above 20°C) the presence of SPEW is indicated by a salinity maximum (Figure 9.12c), while at the lower level (where temperatures are close to 17°C) SPEW salinity is lower than WSPCW salinity (Figure 9.12d).
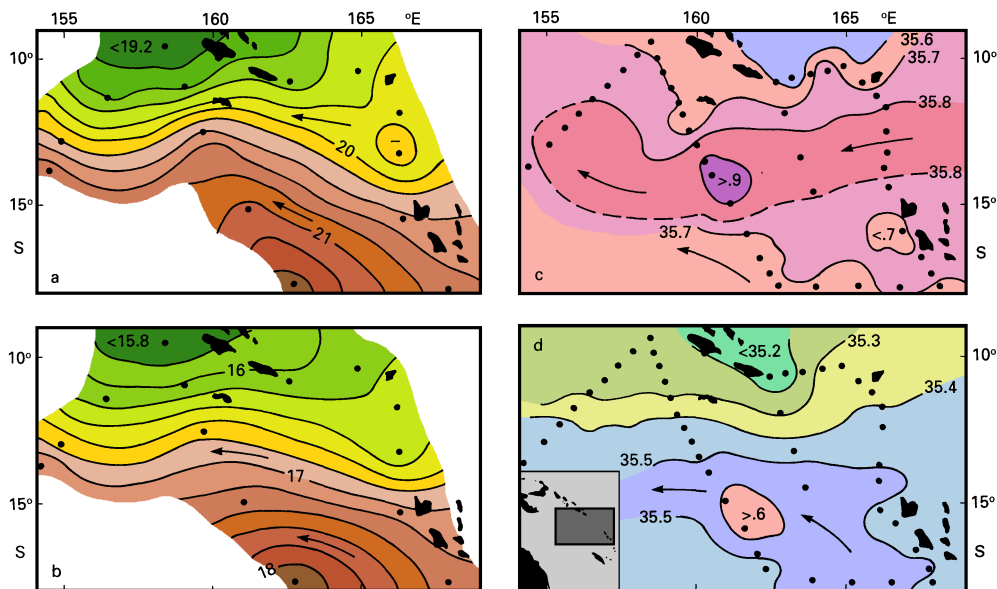


Fig. 9.12. Manifestation of the boundary between SPEW and WSPCW in the eastern Coral Sea. Dynamic height, or steric height multiplied by gravity, relative to an assumed level of no motion of 1200 m, at 148 m (a) and 248 m depth (b), and salinity at 148 m (c) and 248 m depth (d). Arrows give the inferred flow direction. Dots indicate station positions used in drawing the maps; the inset shows the location of the region. From Tomczak and Hao (1989).

The lack of communication between the circulation of the two hemispheres, already demonstrated by last chapter's T-S diagrams of Figure 8.10, produces a distinct separation between SPEW and NPEW along the equator, where the change from one water mass to the other occurs within less than 250 km distance. The change from NPEW to Central Water north of 10°N is more gradual and characterized by a front in which Central Water is found above Equatorial Water, gradually expanding downwards as one proceeds toward north. Observations along 170°W (Figure 9.13) show the transition from NPEW to WNPCW to occur at 200 - 300 m depth near 12°N and at 400 - 600 m near 18°N; north of 20°N the entire thermocline is taken over by WNPCW.
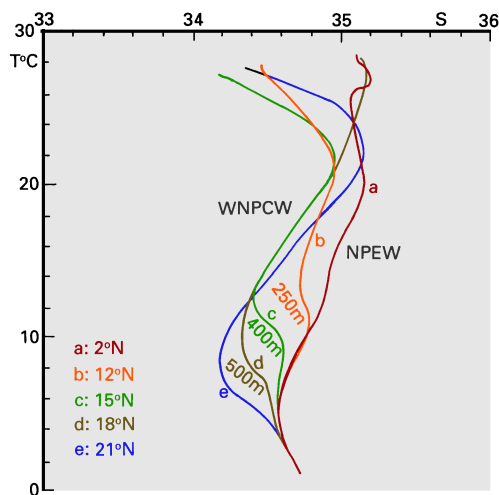


Fig. 9.13. T-S diagrams along 170°W showing the change from NPEW to WNPCW. Data from Osborne *et al*. (1991).

The water of the surface layer south of the southern hemisphere Subtropical Convergence is the Subantarctic Upper Water already discussed in detail in Chapter 6. The equivalent water mass in the northern hemisphere is the *Subarctic Upper Water*. Both water masses are characterized by very low salinities. Some of their water is carried toward the tropics in the eastern boundary currents of the subtropical gyres and mixes with Central Water. The range of T-S combinations produced in the process can be imagined by looking at the range of values spanned by the T-S curves of the Subarctic Upper Water and of ENPCW. Water properties in the transition regions of Figure 9.10 are found in that range. They are the only regions in the world ocean where salinity increases with depth over large parts of the thermocline (usually salinity decreases downwards until the salinity minimum of the Intermediate Water is reached). Examples of T-S curves are given in Figure 9.14.

Main aspects of the hydrographic structure above the permanent thermocline were already discussed in an earlier section of this chapter. A major aspect of surface layer dynamics in the tropical Pacific Ocean is the existence of a barrier layer, particularly in the western region where the layer is a permanent feature. Inspection of Figure 5.7 shows that its existence is closely linked with the Intertropical and South Pacific Convergence Zones (ITCZ and SPCZ), i.e. the location of maximum precipitation. This indicates that in the

western Pacific Ocean the mechanism that creates and maintains the barrier layer is freshening of the surface layer by local rainfall. Figure 9.15 gives an example of the resulting temperature and salinity structure.



Fig. 9.14. T-S diagrams of Central and Subpolar Upper Water and from the "transition region" of Fig. 9.10. Data from Osborne *et al*. (1991).
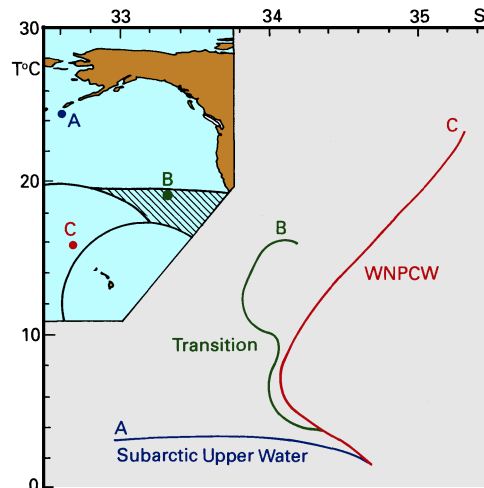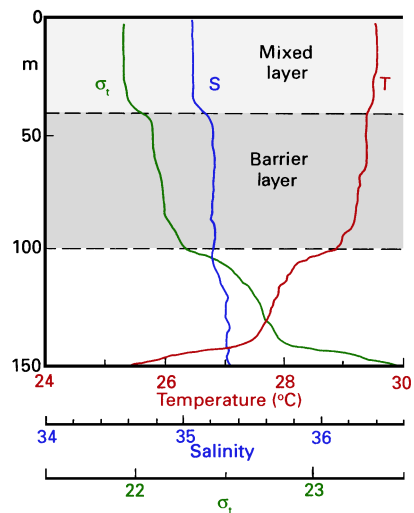


Fig. 9.15. An observation of the barrier layer in the western equatorial Pacific Ocean; *T*: temperature (°C), *S*: salinity. The halocline is above the tropical thermocline, the depth of the mixed layer indicated by the shallower of the two. From Lukas and Lindstrom (1991).

The existence of the barrier layer has only been noted recently and has caused oceanographers and meteorologists to revise some of their ideas about ocean-atmosphere coupling mechanisms. What happens between the ocean and the atmosphere in the western equatorial Pacific Ocean is of utmost importance for the dynamics of the ENSO phenomenon, a major fluctuation of climatic conditions over one half of the globe. The dynamics of ENSO will be discussed in Chapter 19; in the context of barrier layer

dynamics it is sufficient to note that winds tend to blow towards regions of highest sea surface temperature (SST; Figure 2.5a shows that the ITCZ and SPCZ are regions of maximum SST). These high temperatures were traditionally believed to be the product of a net heat flux into the ocean. The heat gained from the atmosphere would raise the temperature of the surface mixed layer until a balance is achieved between heat gain at the surface and heat loss at the bottom of the mixed layer from mixing with colder water. This concept reflects the dynamics of the mixed layer in many regions of the subtropics and temperate zones rather well. It fails in the presence of a barrier layer because the temperature gradient at the bottom of the mixed layer is zero (Figure 9.15), which excludes heat loss through mixing. Horizontal temperature gradients in the western tropical Pacific Ocean are also very small, so countering the heat gain at the surface by bringing in cold water with the currents is also not possible. The conclusion has to be that the net heat flux into the ocean at the surface must be close to zero. This should be compared with the distribution of Figure 1.6 which shows a net heat flux of 40 W m$^2$ for the region in question. This is a low value - earlier heat flux maps give 80 W m$^2$ and more - but still too large to close the oceanic heat budget in the presence of a barrier layer.

The problem lies in the calculation of the various components of the heat budget from observations of so-called bulk parameters, i.e. parameters that do not themselves represent heat fluxes but are easy to measure or estimate, such as air temperature, cloudiness, or wind speed. The formulae used to derive the contributions to the heat budget from long wave back-radiation, evaporation, and direct heat transfer to the atmosphere from bulk parameters are based on semi-empirical arguments and calibrated at moderate to high wind speeds. Winds over the western tropical Pacific Ocean are, however, very light during most parts of the year (Figure 1.2), and the formulae used successfully for other ocean regions may not apply to such calm conditions. Recent measurements of the heat flux terms under low wind speed conditions in the field (Godfrey *et al*., 1991) indicate indeed that under the cloudy sky of the ITCZ and SPCZ in the western equatorial Pacific Ocean the evaporative heat loss is large enough to counter the heat gained by direct solar radiation, and that the net heat transfer between ocean and atmosphere is very small. It is thus very likely that in regions of very low wind speeds the net heat flux values given in Figure 1.6 are much too high. A more detailed discussion of the exchange of properties between the ocean and the atmosphere will be presented in Chapter 18.